

# Effects of Ketamine on Metabolomics of Serum and Urine in Cynomolgus Macaques (*Macaca fascicularis*)

Xueying Pan,<sup>1,2</sup> Xiancheng Zeng,<sup>2</sup> Jiehua Hong,<sup>1</sup> Congli Yuan,<sup>1</sup> Li Cui,<sup>1</sup> Jing Ma,<sup>2</sup> Yan Chang,<sup>2</sup> and Xiuguo Hua<sup>1,\*</sup>

In this study, a metabolomics approach based on nuclear magnetic resonance spectroscopy and pertinent multivariate data analyses was used to evaluate the effect of ketamine on metabolic markers in cynomolgus macaques. Principal component analysis and orthogonal projection to latent structure with discriminant analysis showed that ketamine (10 mg/kg) induced metabolic perturbations. Compared with the control group, ketamine-treated macaques had lower serum levels of  $\alpha$ -glucose, myoinositol, lactate and succinate and lower urine levels of pyruvate and lactate. In contrast, the levels of leucine in serum and arginine in urine were significantly higher in the ketamine group. Our results also demonstrated that a single injection of ketamine influenced the major energy and amino acid metabolic pathways in cynomolgus macaques. Our study suggests that these influences should be considered in the design of experiments and the interpretation related blood and urine data from ketamine-sedated cynomolgus macaques.

**Abbreviations:** NMDA, *N*-methyl-*D*-aspartate; NMR, nuclear magnetic resonance; OPLS-DA, orthogonal projection to latent structure with discriminant analysis

As some of the phylogenetically closest relatives of humans, cynomolgus macaques have increasingly been used in biomedical research, especially in the safety evaluation of new drugs, chemical agents, vaccines, and other substances.<sup>21,23,32,43</sup> Because cynomolgus macaques (especially male animals) can be very aggressive and because training them is time-consuming, immobilization is commonly required.<sup>14,15,24,29</sup> However, physical restraint of animals can induce stress and fear, which can affect the experiment. Currently, alternative options of physical restraint include the addition of psychologic support, the administration of chemical sedatives, and long-term training.

Ketamine is a noncompetitive *N*-methyl-*D*-aspartate (NMDA) receptor antagonist that binds to the phencyclidine receptor and thereby blocks the NMDA receptor channel.<sup>12,37,41</sup> As a chemical immobilization agent, ketamine is commonly used to restrain animals during drug administration, blood collection, physical examination, veterinary diagnosis, and other experimental manipulations in NHP and other laboratory animal species. Despite its frequent use as a sedative, ketamine has many side effects, including interference with recall and recognition memory;<sup>19,35</sup> working memory,<sup>1</sup> and executive function;<sup>22</sup> transient dissociation; the induction of psychotomimetic symptoms, and the stimulation of PRL release and hemodynamic changes (for example, increases in blood pressure).<sup>24</sup> However, whether these side effects are related to the sedative efficacy of ketamine and how they might affect the living biologic system as a whole are unknown.

Metabolomics—a noninvasive, global, nontargeted approach for the investigation of biochemical processes and metabolic networks—has been used to characterize drug metabolic profiles

and biomarkers. This approach requires only small amounts of samples to generate metabolic profiles.<sup>27,31</sup> In our current study, to provide insight into metabolic alterations after ketamine treatment, we combined <sup>1</sup>H nuclear magnetic resonance (NMR) spectroscopy and pertinent multivariate data analyses to detect serum and urine metabolites in cynomolgus macaques.

## Materials and Methods

**Ethics approval.** All procedures were performed in accordance with the Chinese and provincial guidelines for animal welfare.<sup>19,44</sup> The protocol was reviewed and approved by the IACUC of the National Shanghai Center for New Drug Safety Evaluation and Research, which is AAALAC-accredited.

**Animal treatment and sample collection.** Healthy male cynomolgus macaques (age, approximately 5 y; weight, 4.6 ± 0.5 kg) obtained from Hainan Jingang Biotech (animal license no. SCXK [Qiong] 2010-0001; Haikou, Hainan, People's Republic of China) were used in the present study. All macaques were free of *Ceropithecine herpesvirus* type I, simian retrovirus D, SIV, simian T lymphotropic virus type 1, simian pox virus, *Salmonella* spp., *Shigella* spp., *Mycobacterium tuberculosis*, *Yersinia enterocolitica*, *Campylobacter jejuni*, pathogenic dermal fungi, and both exoparasites and endoparasites.

Macaques were individually housed in stainless steel cages (Suzhou Suhuanguang Technology Equipment, Suzhou, People's Republic of China), each with a squeeze board. The temperature in the animal holding room was maintained at 18 to 24 °C, and relative humidity was 40% to 70%; these parameters were recorded automatically every hour by a built-in automatic system. In addition, the animal holding room was maintained on a 12:12-h light:dark cycle (lights on, 0700; intensity, 150 to 300 lx) with 15 to 20 fresh-air changes (100%) hourly. The macaques' normal pelleted feed (Beijing Keao Xieli Feed, Beijing, People's Republic of China) was supplemented with nuts twice each week and with fruits daily, and deionized water was available

Received: 14 Oct 2015. Revision requested: 25 Nov 2015. Accepted: 18 Feb 2016.

<sup>1</sup>Shanghai Key Laboratory of Veterinary Biotechnology, School of Agriculture and Biology, Shanghai Jiaotong University, Shanghai 200240, P.R. China and <sup>2</sup>National Shanghai Center for New Drug Safety Evaluation & Research, Shanghai 201203, P.R. China.

\*Corresponding author. Email: hxg@sjtu.edu.cn

without restriction by bottle in the home cage. Commercial toys (for example, rubber Kong toys [Kong, Golden, CO]) and stainless steel mirrors (Suzhou Suhuang Technology Equipment) were provided to each animal.

In the present study, 12 healthy adult male cynomolgus macaques were randomly allocated into 2 groups: untreated controls ( $n = 6$ ) and ketamine-sedated animals ( $n = 6$ ). Macaques received a single intramuscular dose of either saline (0.2 mL/kg; Sodium Chloride Injection, Qingzhou Yaowang Medicine, Weifang, People's Republic of China) or ketamine (10 mg/kg; 50 mg/mL, Ketamine Hydrochloride Injection, Fujian Gutian Pharm, Gutian, People's Republic of China) in the quadriceps muscle.

Blood samples (2 mL each) were collected by venipuncture of a cephalic vein from conscious control animals and ketamine-sedated macaques at approximately 5 min after full sedation had been achieved and at 24 h after full recovery from sedation. Blood samples were collected through disposable syringes (Shanghai Kindly Enterprise Development Group, Shanghai, People's Republic of China) and added into EDTA-treated serum separator tubes (Sekisui Medical Technology, Beijing, the People's Republic of China). Serum was obtained after centrifugation at 4 °C,  $1000 \times g$  for 10 min and stored at  $-80$  °C until NMR analysis.

Beginning 5 min after treatment, urine samples were collected for 24 h from macaques in metabolic cages (Suzhou Suhuang Technology Equipment). The only difference between the metabolic cages and the normal housing cages is that the metabolic cages had a sloped tray with a central hole for sample collection; otherwise the materials, size and shape of the housing and metabolic cages were the same. A layer of dry ice followed by one of crushed ice was placed around the sterile urine container in the collection box to prevent deterioration of the urine during the 24-h collection process. Urine samples (4 mL each) were collected and stored at  $-80$  °C until analysis. At the end of the study, all animals were returned to colony.

**$^1\text{H-NMR}$  spectroscopy of serum and urine samples.** Urine and serum samples were thawed at room temperature. Samples were allowed to equilibrate at room temperature for 10 min before spectra were acquired. A total of 200  $\mu\text{L}$  of each serum sample was diluted with 400  $\mu\text{L}$  0.9% saline containing 50%  $\text{D}_2\text{O}$  ( $\text{D}_2\text{O}$  was added for a field-locking signal) in 5-mm NMR tubes. Each 550  $\mu\text{L}$  urine sample was centrifuged ( $1000 \times g$ , 5 min, 4 °C) and then diluted with 150  $\mu\text{L}$  1 M sodium phosphate buffer containing 100%  $\text{D}_2\text{O}$  in 5-mm NMR tubes. The external reference containing 1 mM 3-(trimethylsilyl)-propionic acid (Sigma-Aldrich, St Louis, MO) in  $\text{D}_2\text{O}$  was applied in a closed capillary (Wilmad, Buena, NJ). The proton NMR spectra of serum and urine were recorded at 298K on a spectrometer (Avance DRX-600, Bruker Biospin, Rheinstetten, Germany) operated at a  $^1\text{H}$  frequency of 600.11 MHz by using a cryogenic probe. For each serum sample, 3 water-suppressed 1D  $^1\text{H}$  NMR spectra were obtained by using the first increment of the NOESY (standard 1D) pulse sequence (90o-t1-90o-tm-90o-acq), the Carr-Purcell-Meiboom-Gill spin-echo pulse sequence, and a diffusion-edited NMR spectrum by using the bipolar-pair longitudinal-eddy-current pulse sequence to measure large macromolecules such as lipoproteins.  $^1\text{H-NMR}$  spectra were acquired and then processed according to parameters previously published.<sup>3,16</sup> For each urine sample, a water-suppressed 1D  $^1\text{H}$  NMR spectrum was acquired. In brief, the 90° pulse length (approximately 10.0  $\mu\text{s}$ ) was adjusted individually for each sample, followed by 64 transient collections into 32,000 data points for each spectrum with similar spectral widths (20 ppm) and recycle delays (2.0

s). To assign resonance, 2D  $^1\text{H-}^1\text{H}$  correlation spectroscopy<sup>18,20</sup> and total correlation spectroscopy<sup>2</sup> spectra were obtained for selected sera and urine samples.

**Analysis of NMR data.** Free induction decays were multiplied by an exponential filter function equivalent to 1.0 Hz prior to Fourier transformation, and then the spectra were adjusted for phase and baseline distortions manually by using TopSpin 3.0 (Bruker Biospin). Changes in chemical shifts of serum and urine spectra were obvious due to the introduction of a glucose molecule and thus were referenced to the anomeric proton of  $\alpha$ -glucose at  $\delta$  5.23 and the methyl of 3-(trimethylsilyl)-propionic acid at  $\delta$  0, respectively.

NMR spectra in serum ( $\delta$  0.5 to 8.5) and urine ( $\delta$  0.5 to 9.5) were integrated by using the AMIX package (version 3.8.3, Bruker Biospin), and each region was 0.002 ppm wide. The water regions in serum ( $\delta$  4.55 to 5.13) and urine ( $\delta$  4.70 to 5.05) were removed to prevent the effects of imperfect water suppression, the urea peaks ( $\delta$  5.6 to 6.03) were removed from the urine spectra. Subsequently, the data were normalized to the remaining integral regions for each spectrum prior to pattern recognition analysis.

To investigate inherent differences in the samples, principal component analysis was conducted on both the serum and urine samples by using Simca-P 11.0 software (Umetrics, Malmo, Sweden).<sup>3</sup> NMR spectral data were further analyzed according to the orthogonal projection to latent structure with discriminant analysis (OPLS-DA) method with unit variance scaling to maximize the separation in the samples.<sup>4,36</sup> The findings were imported into Excel (Microsoft, Redmond, WA) and then plotted as color-coded absolute coefficient values ( $|r|$ ) of the variables by using MATLAB (MathWorks, Natick, MA).<sup>5</sup> The color coding corresponds to the coefficients of the resonances within the classes. A correlation coefficient of  $|r| > 0.75$  was regarded as significant on the basis of the significance of discrimination at the level of  $P$  less than 0.05 determined according to Pearson correlation coefficient. The OPLS-DA models were validated by using the full cross-validation method and a permutation test.<sup>8,17,26,42,47</sup> The quality of the models was evaluated by using  $R^2X$ , corresponding to the goodness of fit, and  $Q$ ,<sup>11</sup> defining the predictive ability. Because the results of OPLS-DA from the spin-echo and diffusion-edited NMR spectra for serum were similar to those obtained for the standard 1D NMR spectra, the analysis of diffusion-edited NMR spectra will not be discussed in the Results.

## Results

**$^1\text{H}$  NMR spectra of serum and urine samples.** We determined the metabolic profiles of the control and ketamine-sedated macaques by measuring the 1D  $^1\text{H}$  NMR spectra of serum and urine samples. Examples of typical  $^1\text{H}$  NMR spectra from the serum and urine of a control macaque are shown in Figure 1. About 50 metabolites in urine and serum from these spectra were unambiguously assigned. The corresponding  $^1\text{H}$  NMR chemical shifts, signal multiplicities, families, and compartments are shown in Table 1. A total of 26 identified metabolites were present in both urine and serum: leucine, alanine, isoleucine, lysine, valine, glutamate, citrate, phenylalanine, arginine, lactate, fumarate, acetate, 1-methylhistidine, creatine, creatinine,  $\alpha$ -glucose, glutamine, succinate, threonine,  $\beta$ -glucose, formate, trimethylamine, trimethylamine N-oxide, urea, myoinositol, and glycoprotein. Another 12 metabolites were present in urine but not serum: 3-hydroxybutyrate, betaine, hippurate, taurine, 3-hydroxyisobutyrate, dimethylamine,  $\alpha$ -ketoglutarate, acetoacetate, allantoin, phenylacetyl-glycine, *trans*-aconitate, and

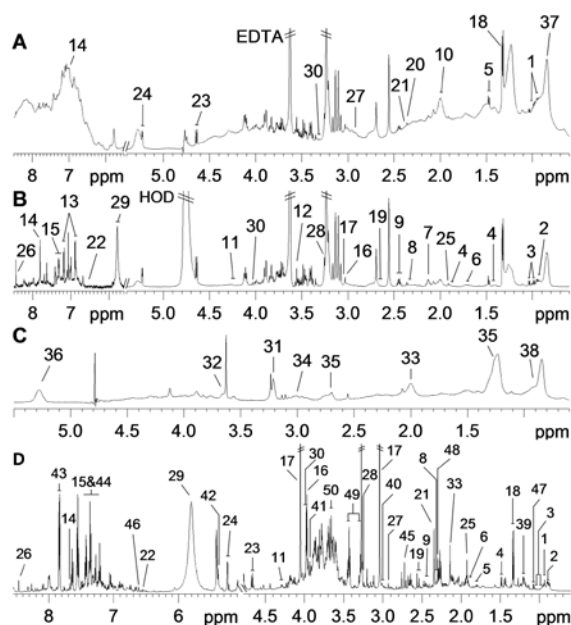


**Figure 1.** Typical NMR spectra of serum and urine samples from a control cynomolgus macaque. (A) Carr-Purcell-Meiboom-Gill  $^1\text{H}$  NMR spectrum of metabolites from serum samples. (B) Standard 1D  $^1\text{H}$  NMR spectrum of metabolites from serum samples. (C) Bipolar-pair longitudinal-eddy-current  $^1\text{H}$  NMR spectrum of metabolites from serum samples. (D) Standard 1D  $^1\text{H}$  NMR spectrum of metabolites from urine samples. Spectra in the aromatic region ( $\delta$  5.6–8.5) were magnified (A) 16 times or (B) 4 times compared with the aliphatic region ( $\delta$  0.6–5.4); (D) the spectra in the aromatic region ( $\delta$  5.1–8.5) were magnified 4 times compared with the aliphatic region ( $\delta$  0.6–4.7). Chemical shifts and peak multiplicities of key metabolites are listed in Table 1.

unknown. In addition, 12 metabolites were unique to serum: methionine, pyruvate, proline, tyrosine, choline, glycine, albumin, lipids (triglycerides and fatty acids), glycerylphosphorylcholine, unsaturated lipids, LDL, and VLDL. The assignment of metabolites in urine and serum was based on published data<sup>16,17,47</sup> and further confirmed by 2D  $^1\text{H}$ - $^1\text{H}$  correlation and total correlation spectroscopy (data not shown). Visual inspection of the  $^1\text{H}$  NMR spectra showed visible differences in serum and urine metabolites. All signals from observable metabolites were contained in the standard 1D NMR spectrum. To distinguish the signals from small metabolites, such as amino acids and lipid metabolites in serum, a spin-echo pulse NMR sequence was used.

**OPLS-DA analysis of urine and serum samples.** OPLS-DA was conducted to detect metabolic changes in the serum and urine samples. OPLS-DA scores (Figure 2) showed that the distribution areas of the 24-h samples for the 2 groups were completely separated and that the metabolic components in the serum and urine of cynomolgus macaques were significantly different. This analysis yielded  $R^2X = 0.61$ ,  $R^2Y = 0.93$ ,  $Q^2 = 0.53$  for serum samples and  $R^2X = 0.38$ ,  $R^2Y = 0.79$ ,  $Q^2 = 0.57$  for urine samples. The degrees of difference were analyzed according to the chemical shift of the different metabolic components in the ketamine-treated and control groups received from the coefficients of correlation that were gained from the comparison and analysis of the 2 sets of OPLS-DA data. The different metabolic components at 24 h after treatment also were analyzed by using  $^1\text{H}$ - $^1\text{H}$  associated with nuclear spectrum (correlation spectroscopy spectra) technologies (Table 2).

The corresponding coefficient plot showed that serum levels of lactate,  $\alpha$ -glucose, and myoinositol were lower ( $P < 0.05$ ) in the ketamine group than the control group, whereas the serum level of arginine was higher ( $P < 0.05$ ) in the ketamine-sedated

than control macaques (Figure 2). The multivariate data analysis indicated that urine levels of leucine were higher ( $P < 0.05$ ) but those of lactate, pyruvate, and succinate were lower ( $P < 0.05$ ) in ketamine-treated compared with control animals (Figure 2).

## Discussion

Ketamine is a noncompetitive antagonist of the NMDAR and was developed in the 1960s as a safer anesthetic alternative to phencyclidine.<sup>10,11,33,41</sup> Ketamine has been used for the induction and maintenance of general anesthesia for more than 50 y and is generally considered a safe anesthetic. Ketamine has also been used widely for the sedation of NHP, including cynomolgus macaques. Reported undesirable central effects of ketamine in patients anesthetized with ketamine include hallucinogenic and dissociative experiences, and it therefore has been prohibited for pediatric, geriatric, and veterinary anesthesia.<sup>41</sup> Some studies also reported symptoms of dissociation and hallucinations, which were usually transient.<sup>30,44,45,48</sup> A recent study, in which 10 patients with obsessive-compulsive disorder received ketamine, reported an increase in anxiety and suicidal thoughts in 2 patients.<sup>28</sup> Ketamine is rapidly metabolized by hepatic microsomal enzymes CYP3A4 into a series of compounds, among which norketamine and hydroxynorketamine are considered the most important.<sup>41</sup>

In the current study, serum levels of lactate,  $\alpha$ -glucose, and myoinositol and urine levels of lactate, pyruvate, and succinate were decreased in the ketamine group as compared with the control group. These compounds belong to the glycolysis-gluconeogenesis pathway, thus suggesting its interference by ketamine. Previous data from a study in rats suggested that the antidepressant-like effect observed after a single injection of ketamine was mediated by an increased anabolic rate-mediating cell growth and differentiation.<sup>40</sup>

The decreased levels of lactate, pyruvate, succinate, myoinositol, and  $\alpha$ -glucose might suggest increased anabolism and activity of the glycolytic pathway. These findings were in accordance with previous results,<sup>40</sup> in which almost all metabolites of this pathway showed lower levels after a single injection of ketamine in mice. These changes might be due to a feedback mechanism of the tricarboxylic acid pathway, with consequent effects (positive or negative) on glycolysis, or to changes in the ratios of metabolites in the glycolysis pathway, which reflect altered enzyme activities or protein expression.

Ketamine blocks the NMDAR resulting in a decreased  $\text{Ca}^{2+}$  flux into cells and mitochondria, perhaps ultimately leading to the inactivation of related enzymes and altering metabolite levels.<sup>13,40</sup> Here, the decreased pyruvate level might be mediated, at least in part, by the decrease in glucose. Alternatively, the decreased levels of myoinositol in serum might suggest an alteration in serum osmolarity, given that myoinositol is an important intracellular osmolyte<sup>17</sup>. Moreover, inositol, a carbocyclic polyol, provides the structural basis for many secondary messengers (including phosphatidylinositol, inositol phosphates, and phosphatidylinositol phosphate) in eukaryotic cells. Inositols are organic osmolytes and are often associated with the regulation of intracellular calcium concentration, insulin signal transduction, and oxidation of fatty acids.<sup>9,17,25</sup>

When insufficient glucose is available, marked levels of acetoacetyl CoA are generated from ketogenic amino acids (for example, leucine) through oxidative decarboxylation of pyruvic acid and are converted into ketones in the liver. Amino acids that are both glucogenic and ketogenic, such as tryptophan and isoleucine, can participate in several metabolic pathways to supplement blood glucose or to synthesize

**Table 1.** Assignment of serum and urine metabolites in cynomolgus macaques according to chemical shifts relative to the doublet of  $\alpha$ -glucose ( $\delta$  5.23) and the methyl of sodium 3-(trimethylsilyl) propionate ( $\delta$  0)

	Metabolite	Moieties	$\delta$ $^1\text{H}$ (ppm) and multiplicity	Compound	Compartments
1	Leucine	$\alpha\text{CH}$ , $\beta\text{CH}_2$ , $\gamma\text{CH}$ , $\delta\text{CH}_3$ , $\delta\text{CH}_3$	3.72 (t), 1.96 (m), 1.63 (m), 1.69 (m), 0.91 (d), 0.96 (d)	Amino acid	serum, urine
2	Alanine	$\alpha\text{CH}$ , $\beta\text{CH}_3$	3.77 (q), 1.48 (d)	Amino acid	serum, urine
3	Isoleucine	$\alpha\text{CH}$ , $\beta\text{CH}$ , $\gamma\text{CH}_2$ , $\gamma\text{CH}_3$ , $\delta\text{CH}_3$	3.65 (d), 1.95 (m), 1.25 (m)-1.45 (m), 1.01 (d), 0.94 (t)	Amino acid	serum, urine
4	Lysine	$\alpha\text{CH}$ , $\beta\text{CH}_2$ , $\gamma\text{CH}_2$ , $\delta\text{CH}_2$ , $\epsilon\text{CH}_2$	3.77 (t), 1.89 (m), 1.73 (m), 1.44 (m), 3.01 (t)	Amino acid	serum, urine
5	Valine	$\alpha\text{CH}$ , $\beta\text{CH}$ , $\gamma\text{CH}_3$	3.61 (d), 2.26 (m), 0.98 (d), 1.04 (d)	Amino acid	serum, urine
6	Methionine	$\alpha\text{CH}$ , $\beta\text{CH}_2$ , $\gamma\text{CH}_2$ , $\delta\text{CH}_3$	3.78 (m), 2.16 (m), 2.63 (dd), 2.14 (s)	Amino acid	serum
7	Glutamate	$\alpha\text{CH}$ , $\beta\text{CH}_2$ , $\gamma\text{CH}_2$	3.75 (m), 2.08 (m), 2.35 (m)	Amino acid	serum, urine
8	Citrate	half $\text{CH}_2$ , half $\text{CH}_2$	2.52 (d), 2.68 (d)	Tricarboxylic acid	serum, urine
9	Phenylalanine	2, 6-CH, 3,5-CH, 4-CH	7.33 (m), 7.38 (m), 7.42 (m)	Amino acid	serum, urine
10	Pyruvate	$\text{CH}_3$	2.37 (s)	Carboxylic acid (keto acid)	serum
11	Arginine	$\alpha\text{CH}$ , $\beta\text{CH}_2$ , $\gamma\text{CH}_2$ , $\delta\text{CH}_2$	3.76 (t), 1.89 (m), 1.63 (m), 3.25 (t)	Amino acid	serum, urine
12	Lactate	$\alpha\text{CH}$ , $\beta\text{CH}_3$	4.11 (q), 1.33 (d)	Carboxylic acid (hydroxy acid)	serum, urine
13	Fumarate	CH	6.52 (s)	Dicarboxylic acid	serum, urine
14	Acetate	$\text{CH}_2\text{-C}=\text{O}$	1.92 (s)	Dicarboxylic acid	serum, urine
15	1-Methylhistidine	4-CH, 2-CH	7.05 (s), 7.75 (s),	Amino acid derivative	serum, urine
16	Proline	$\alpha\text{CH}$ , $\beta\text{CH}_2$ , $\gamma\text{CH}_2$ , $\delta\text{CH}_2$	4.11 (t), 2.02 (m)-2.33 (m), 2.00 (m), 3.35 (t)	Amino acid	serum
17	Creatine	N- $\text{CH}_3$ , $\text{CH}_2$	3.03 (s), 3.93 (s)	Amino acid derivative	serum, urine
18	Tyrosine	CH, CH	7.19 (m), 6.89 (m)	Amino acid	serum
19	3-Hydroxybutyrate	$\text{CH}_3$	1.20 (d)	Carboxylic acid (keto acid)	urine
20	Creatinine	$\text{CH}_3$ , $\text{CH}_2$	3.04 (s), 4.05 (s),	Amino acid derivative	serum, urine
21	$\alpha$ -Glucose	1-CH	5.24 (d)	Carbohydrate	serum, urine
22	Glutamine	$\alpha\text{CH}$ , $\beta\text{CH}_2$ , $\gamma\text{CH}_2$	3.68 (t), 2.15 (m), 2.45 (m)	Amino acid	serum, urine
23	Succinate	$\alpha$ , $\beta\text{CH}_2$	2.40 (s)	Carboxylic acid	serum, urine
24	Choline	N-( $\text{CH}_3$ ) $_3$ , $\alpha\text{CH}_2$ , $\beta\text{CH}_2$	3.2 (s), 4.05 (t), 3.51 (t)	Lipid	serum
25	Glycine	$\text{CH}_2$	3.56 (s)	Amino acid	serum
26	Threonine	$\alpha\text{CH}$ , $\beta\text{CH}$ , $\gamma\text{CH}_3$	3.58 (d), 4.24 (m), 1.32 (d)	Amino acid	serum, urine
27	Albumin	Lysyl- $\text{CH}_2$	3.02	Protein	serum
28	$\beta$ -Glucose	1-CH	4.65 (d)	Carbohydrate	serum, urine
29	Formate	CH	8.45 (s)	Carboxylic acid	serum, urine
30	Trimethylamine	$\text{CH}_3$	2.92 (s)	Exogenous	serum, urine
31	Trimethylamine N oxide	$\text{CH}_3$	3.26 (s)	Exogenous	serum, urine
32	Lipids (triglycerides and fatty acids)	$\text{CH}_3(\text{CH}_2)_{n'}$ , $(\text{CH}_2)_{n'}$ , $\text{CH}_2\text{-CH}_2\text{CO}$ , $\text{CH}_2\text{-C}=\text{C}$ , $\text{CH}_2\text{-C}=\text{O}$ , $\text{CH-O-CO}$	1.22 (m), 1.29 (m), 1.58 (m), 2.04 (m), 2.24 (m), 2.75 (m)	Lipid	serum
33	Urea	$\text{NH}_2$	5.78 (s)	Amino acid derivative	serum, urine
34	Betaine	$\text{CH}_2$ , $\text{CH}_3$	3.9 (s), 3.27 (s)	Amino acid derivative	urine
35	Myoinositol	5-CH, 4, 6-CH, 1, 3-CH, 2-CH	3.30 (t), 3.63 (t), 3.53 (dd), 4.06 (t)	Carbohydrate	serum, urine
36	Glycerophosphorylcholine	N-( $\text{CH}_3$ ) $_3$ , $\text{OCH}_2$ , $\text{NCH}_2$	3.22 (s), 4.20 (t), 3.68 (t)	Lipid	serum
37	Glycoprotein	$\text{CH}_3\text{-C}=\text{O}$	2.05 (s), 2.08 (s), 2.15 (s)	Amino acid derivative	serum, urine
38	Hippurate	1-CH, 2-CH, 3-CH	7.8 (d), 7.62 (t), 7.53 (t)	Exogenous	urine
39	Unsaturated lipids	$=\text{C-CH}_2\text{-C}=\text{}$ , $-\text{CH}=\text{CH-}$	5.19 (m), 5.31 (m)	Lipid	serum

Table 1. Continued

	Metabolite	Moieties	$\delta^1\text{H}$ (ppm) and multiplicity	Compound	Compartments
40	Low-density lipoprotein	$\text{CH}_3, (\text{CH}_2)_n$	0.84 (t)	Lipid	serum
41	Taurine	$\text{CH}_2\text{SO}_3, \text{NCH}_2$	3.25 (t), 3.43 (t)	Amino acid	urine
42	Very low-density lipoprotein	$\text{CH}_3^*\text{CH}_2\text{CH}_2\text{C}=\text{}$	0.88 (t)	Lipid	serum
43	3-Hydroxyisobutyrate	$\text{CH}_3$	1.08 (d)	Carboxylic acid (keto acid)	urine
44	Dimethylamine	$\text{CH}_3$	2.72 (s)	Exogenous	urine
45	$\alpha$ -Ketoglutarate	$\text{CH}_2, \text{CH}_2$	3.01 (t), 2.45 (t)	Carboxylic acid	urine
46	Acetoacetate	$\text{CH}_3, \text{CH}_2$	2.30 (s), 3.45 (s)	Carboxylic acid (keto acid)	urine
47	Allantoin	CH	5.41 (s)	Amino acid derivative	urine
48	Phenylacetyl-glycine	NH, 2,6-CH, 3,5-CH, 7-CH, 10-CH	8.00 (s), 7.43 (m), 7.37 (m), 3.75 (d), 3.68 (s)	Amino acid derivative	urine
49	trans-Aconitate	CH, $\text{CH}_2$	6.60 (s), 3.47 (s)	Carboxylic acid	urine
50	Unknown	—	3.63 (m)	—	urine

d, doublet; dd: doublet of doublets; m, multiplet; q, quartet; s, singlet; t, triplet

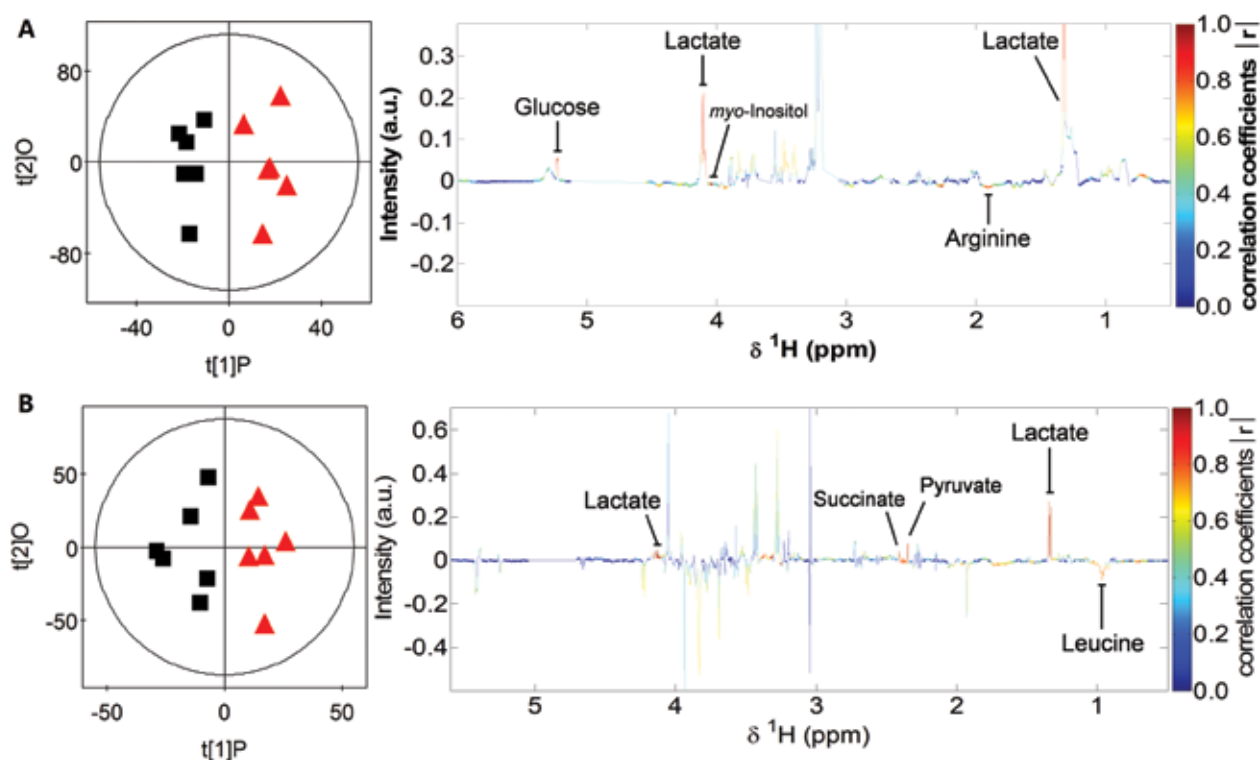


Figure 2. Orthogonal projection to latent structure with discriminant analysis (OPLS-DA) of serum and urine metabolic profiles after ketamine sedation of cynomolgus macaques. (A) Scores (left) and coefficient plots (right) acquired from standard 1D spectra of serum samples from ketamine-treated (red triangles) and control (black squares) macaques ( $R^2X = 0.61$ ,  $R^2Y = 0.93$ ,  $Q^2 = 0.53$ ); (B) Scores (left) and coefficient plots (right) obtained from standard 1D spectra of urine samples from ketamine-sedated (red triangles) and control (black squares) macaques ( $R^2X = 0.38$ ,  $R^2Y = 0.79$ ,  $Q^2 = 0.57$ ). The coefficient plot shows the relative contributions of various metabolites to the differentiation of classes of interest (red > blue).

ketones. However, in our study, the increased concentrations of arginine in serum and of leucine in urine of ketamine-treated macaques might indicate metabolic derangements involving either protein synthesis or amino acid degradation. Ketogenesis might result from a lack of glucose in cynomolgus macaques treated with ketamine, given that ketamine induces loss of appetite and subsequently decreased food consumption in NHP<sup>6</sup> and loss of appetite, nausea, and vomiting in patients with diabetic polyneuropathy and postherpetic neuralgia.<sup>7</sup> The brain can extract and use ketone bodies during starvation and insufficient glucose.<sup>34</sup>

A previous study<sup>38</sup> showed that there were distinct metabolomics differences between responders and nonresponders after treatment of ketamine in humans. Affected metabolites included decanamide, deoxytetradecasphingine, dihydrobenzenediol, dimethyldioxododecatrienal, hexadienoic acid, hexenedial, hydroxyl-hexadienal, oxohexenal, pentadecatetraenal, phenyllactic acid, and phenylvaleric acid. A majority of these metabolites are in the fatty acyl family. In the present study involving cynomolgus macaques, the different metabolites between the 2 groups were myoinositol, lactate, succinate, pyruvate, leucine, and arginine—most of which are components

**Table 2.** Significant differences in orthogonal projection to latent structure with discriminant analysis (OPLS-DA) coefficients of serum and urine metabolites between ketamine-sedated and control cynomolgus macaques

Metabolite ( $\delta$ )	OPLS-DA coefficient (r)	
	Serum	Urine
Leucine (0.96)		0.76
Arginine (2.15)	0.83	
Lactate (1.33)	-0.75	-0.85
Pyruvate (2.37)		-0.86
Succinate (2.40)		-0.88
Myoinositol (4.06)	-0.80	
$\alpha$ -Glucose (5.24)	-0.76	

Positive and negative signs indicate positive and negative correlations in the concentrations of the serum and urine metabolites at 24 h in the ketamine group compared with the control group. A coefficient of 0.75 was used as the cutoff value for significance ( $P < 0.05$ ); blank cells indicate  $r < 0.75$ .

of the tricarboxylic acid cycle. Therefore, responders and non-responders among cynomolgus macaques after treatment of ketamine were difficult to identify. Further studies are needed to better describe the existence and differences between treatment responders and nonresponders.

The biologic half-life of ketamine is 2.5 to 3 h, and more than 99% of the ketamine dose is eliminated within 24 h. Moreover, the metabolites in 24-h urine samples of adult animals are relatively stable, and principal component analysis failed to reveal differences.<sup>39</sup> In addition, biologic rhythm might be a source of experimental errors.<sup>46</sup> Therefore, to minimize interference due to biologic rhythm and differences between individual macaques, urine samples from each animal were collected over 24 h.

However, a few limitations might have influenced the study results. The collection of serum samples from conscious cynomolgus macaques is a potential cause of stress. Therefore, to minimize stress, the procedure was performed by a skilled technician who was familiar with the animals and who collected all of the samples. In addition, all of the animals were acclimated to the blood sampling process before the study. In the present study, serum metabolomics did not differ significantly between the fully sedated macaques and the conscious control group at approximate 5 min after treatment, suggesting that the blood collection process did not induce the observed changes in metabolite levels.

In conclusion, the results of our study showed clear differences in serum and urine metabolite levels between ketamine-sedated and control cynomolgus macaques, suggesting that ketamine affects energy and amino acid metabolism. These effects should be considered in the design of experiments and interpretation of blood or urine data from cynomolgus macaques under ketamine sedation. Furthermore, NMR-based metabolomics were a useful tool in elucidating the effects of ketamine in cynomolgus macaques.

## Acknowledgments

This work was financially supported by the Shanghai Municipal Science and Technology Commission (grant no. 12140903800). We thank Dr Qinghua He for his helpful assistance regarding NMR measurement. We also thank Drs Youjia Hu, Xiaoping Zhao, and Jiaqin Yao for their review of the manuscript.

## References

- Adler CM, Goldberg TE, Malhotra AK, Pickar D, Breier A. 1998. Effects of ketamine on thought disorder, working memory, and semantic memory in healthy volunteers. *Biol Psychiatry* 43:811–816.
- Bax A, Davis DG. 1985. Practical aspects of 2D transverse NOE spectroscopy. *J Magn Reson* 63:207–213.
- Beckonert O, Keun HC, Ebbels TM, Bundy J, Holmes E, Lindon JC, Nicholson JK. 2007. Metabolic profiling, metabolomic, and metabolomic procedures for NMR spectroscopy of urine, plasma, serum, and tissue extracts. *Nat Protoc* 2:2692–2703.
- Bjerrum JT, Wang Y, Hao F, Coskun M, Ludwig C, Gunther U, Nielsen OH. 2014. Metabolomics of human fecal extracts characterize ulcerative colitis, Crohn's disease, and healthy individuals. *Metabolomics* 11:122–133.
- Cloarec O, Dumas ME, Craig A, Barton RH, Trygg J, Hudson J, Blancher C, Gauguier D, Lindon JC, Holmes E, Nicholson J. 2005. Statistical total correlation spectroscopy: an exploratory approach for latent biomarker identification from metabolic <sup>1</sup>H-NMR data sets. *Anal Chem* 77:1282–1289.
- Crockett CM, Shimoji M, Bowden DM. 2000. Behavior, appetite, and urinary cortisol responses by adult female pigtailed macaques to cage size, cage level, room change, and ketamine sedation. *Am J Primatol* 52:63–80.
- Cvrcek P. 2008. Side effects of ketamine in the long-term treatment of neuropathic pain. *Pain Med* 9:253–257.
- Davis VW, Schiller DE, Eurich D, Sawyer MB. 2012. Urinary metabolomic signature of esophageal cancer and Barrett's esophagus. *World J Surg Oncol* 10:271.
- Di Paolo G, De Camilli P. 2006. Phosphoinositides in cell regulation and membrane dynamics. *Nature* 443:651–657.
- Domino EF. 1992. Chemical dissociation of human awareness: focus on noncompetitive NMDA receptor antagonists. *J Psychopharmacol* 6:418–424.
- Dutta A, McKie S, Deakin JF. 2015. Ketamine and other potential glutamate antidepressants. *Psychiatry Res* 225:1–13.
- Fisher K, Coderre TJ, Hagen NA. 2000. Targeting the N-methyl-D-aspartate receptor for chronic pain management. Preclinical animal studies, recent clinical experience, and future research directions. *J Pain Symptom Manage* 20:358–373.
- Gideons ES, Kavalali ET, Monteggia LM. 2014. Mechanisms underlying differential effectiveness of memantine and ketamine in rapid antidepressant responses. *Proc Natl Acad Sci U S A* 111:8649–8654.
- Girard-Buttoz C, Heistermann M, Rahmi E, Agil M, Fauzan PA, Engelhardt A. 2014. Costs of mate guarding in wild male long-tailed macaques (*Macaca fascicularis*): physiologic stress and aggression. *Horm Behav* 66:637–648.
- Gografe SI, Hansen BC, Hansen KD. 2015. Deep subconjunctival injection of gentamicin for the treatment of bacterial conjunctivitis in macaques (*Macaca mulatta* and *Macaca fascicularis*). *Lab Anim (NY)* 44:92–96.
- He Q, Kong X, Wu G, Ren P, Tang H, Hao F, Huang R, Li T, Tan B, Li P, Tang Z, Yin Y, Wu Y. 2008. Metabolomic analysis of the response of growing pigs to dietary L-arginine supplementation. *Amino Acids* 37:199–208.
- He Q, Ren P, Kong X, Xu W, Tang H, Yin Y, Wang Y. 2011. Intrauterine growth restriction alters the metabolome of the serum and jejunum in piglets. *Mol Biosyst* 7:2147–2155.
- He Q, Tang H, Ren P, Kong X, Wu G, Yin Y, Wang Y. 2011. Dietary supplementation with L-arginine partially counteracts serum metabolome induced by weaning stress in piglets. *J Proteome Res* 10:5214–5221.
- Hetem LA, Danion JM, Diemunsch P, Brandt C. 2000. Effect of a subanesthetic dose of ketamine on memory and conscious awareness in healthy volunteers. *Psychopharmacology (Berl)* 152:283–288.
- Hurd RE. 2011. Gradient-enhanced spectroscopy. *J Magn Reson* 213:467–473.
- Kim CY, Han JS, Suzuki T, Han SS. 2005. Indirect indicator of transport stress in hematological values in newly acquired cynomolgus monkeys. *J Med Primatol* 34:188–192.

22. Krystal JH, Bennett A, Abi-Saab D, Belger A, Karper LP, D'Souza DC, Lipschitz D, Abi-Dargham A, Charney DS. 2000. Dissociation of ketamine effects on rule acquisition and rule implementation: possible relevance to NMDA receptor contributions to executive cognitive functions. *Biol Psychiatry* 47:137–143.
23. Ku WW, Pagliusi F, Foley G, Roesler A, Zimmerman T. 2010. A simple orchidometric method for the preliminary assessment of maturity status in male cynomolgus monkeys (*Macaca fascicularis*) used for nonclinical safety studies. *J Pharmacol Toxicol Methods* 61:32–37.
24. Malaivijitnond S, Varavudhi P. 1996. Effect of ketamine anesthesia on serum prolactin levels in male cynomolgus monkeys (*Macaca fascicularis*). *J Sci Soc Thailand* 22:285–297.
25. Mebarek S, Abousalham A, Magne D, Do Le D, Bandorowicz-Pikula J, Pikula S, Buchet R. 2013. Phospholipases of mineralization competent cells and matrix vesicles: roles in physiologic and pathologic mineralizations. *Int J Mol Sci* 14: 5036–5129
26. Mundt F, Johansson HJ, Forshed J, Arslan S, Metintas M, Dobra K, Lehtio J, Hjerpe A. 2013. Proteome screening of pleural effusions identifies galectin as a diagnostic biomarker and highlights several prognostic biomarkers for malignant mesothelioma. *Mol Cell Proteomics* 13:701–715.
27. Nicholson JK, Holmes E, Kinross JM, Darzi AW, Takats Z, Lindon JC. 2012. Metabolic phenotyping in clinical and surgical environments. *Nature* 491:384–392.
28. Niciu MJ, Grunsel BD, Corlett PR, Pittenger C, Bloch MH. 2013. Two cases of delayed-onset suicidal ideation, dysphoria, and anxiety after ketamine infusion in patients with obsessive-compulsive disorder and a history of major depressive disorder. *J Psychopharmacol* 27:651–654.
29. Reinhardt V. 2003. Working with rather than against macaques during blood collection. *J Appl Anim Welf Sci* 6:189–197.
30. Reinstatler L, Youssef NA. 2015. Ketamine as a potential treatment for suicidal ideation: a systematic review of the literature. *Drugs R D* 15:37–43.
31. Shajahan-Haq AN, Cheema MS, Clarke R. 2015. Application of metabolomics in drug-resistant breast cancer research. *Metabolites* 5:100–118.
32. Sibal LR, Samson KJ. 2001. Nonhuman primates: a critical role in current disease research. *ILAR J* 42:74–84.
33. Sleigh J, Harvey M, Voss L, Denny B. 2014. Ketamine—more mechanisms of action than just NMDA blockade. *Trends in anaesthesia and critical care* 4:76–81.
34. Sokoloff L. 1973. Metabolism of ketone bodies by the brain. *Annu Rev Med* 24:271–280.
35. Taffe MA, Davis SA, Gutierrez T, Gold LH. 2002. Ketamine impairs multiple cognitive domains in rhesus monkeys. *Drug Alcohol Depend* 68:175–187.
36. Trygg J, Wold S. 2002. Orthogonal projections to latent structures (O PLS). *J Chemom* 16:119–128.
37. van Velzen M, Dahan A. 2014. Ketamine metabolomics in the treatment of major depression. *Anesthesiology* 121:4–5.
38. Villaseñor A, Ramamoorthy A, Silva dos Santos M, Lorenzo MP, Laje G, Zarate C Jr, Barbas C, Wainer IW. 2014. A pilot study of plasma metabolomic patterns from patients treated with ketamine for bipolar depression: evidence for a response-related difference in mitochondrial networks. *Br J Pharmacol* 171:2230–2242.
39. Wang XY. [Internet]. 2007. Metabonomic study on the acute and chronic stresses and drug intervention. PhD dissertation. Shanghai Jiaotong University, Shanghai, China. [Cited 10 August 2016]. Available at: <http://cdmd.cnki.com.cn/Article/CDMD-10248-2008052192.htm>. [Article in Chinese]
40. Weckmann K, Labermaier C, Asara JM, Müller MB, Turck CW. 2014. Time-dependent metabolomic profiling of ketamine drug action reveals hippocampal pathway alterations and biomarker candidates. *Transl Psychiatry* 4:e481.
41. Wen C, Zhang M, Ma J, Hu L, Wang X, Lin G. 2015. Urine metabolomics in rats after administration of ketamine. *Drug Des Devel Ther* 9:717–722.
42. Xiao H, Jiang N, Schaffner E, Stockinger EJ, van der Knaap E. 2008. A retrotransposon-mediated gene duplication underlies morphological variation of tomato fruit. *Science* 319:1527–1530.
43. Xie L, Zhou Q, Liu S, Wu Q, Ji Y, Zhang L, Xu F, Gong W, Melgiri ND, Xie P. 2014. Normal thoracic radiographic appearance of the cynomolgus monkey (*Macaca fascicularis*). *PLoS One* 9:e84599.
44. Zarate CA Jr, Brutsche NE, Ibrahim L, Franco-Chaves J, Diazgranados N, Cravchik A, Selter J, Marquardt CA, Liberty V, Luckenbaugh DA. 2012. Replication of ketamine's antidepressant efficacy in bipolar depression: a randomized controlled add-on trial. *Biol Psychiatry* 71:939–946.
45. Zarate CA Jr, Singh JB, Carlson PJ, Brutsche NE, Ameli R, Luckenbaugh DA, Charney DS, Manji HK. 2006. A randomized trial of an N-methyl-D-aspartate antagonist in treatment-resistant major depression. *Arch Gen Psychiatry* 63:856–864.
46. Zeng XC, Yang CM, Pan XY, Yao YS, Pan W, Zhou C, Jiang ZR, Chang Y, Ma J. 2010. Effects of fasting on hematologic and clinical chemical values in cynomolgus monkeys (*Macaca fascicularis*). *J Med Primatol* 40:21–26.
47. Zhang X, Wang Y, Hao F, Zhou X, Han X, Tang H, Ji L. 2009. Human serum metabonomic analysis reveals progression axes for glucose intolerance and insulin resistance statuses. *J Proteome Res* 8:5188–5195.
48. Zigman D, Blier P. 2013. Urgent ketamine infusion rapidly eliminated suicidal ideation for a patient with major depressive disorder: a case report. *J Clin Psychopharmacol* 33:270–272.